Nanoscale

COMMUNICATION

View Article Online
View Journal | View Issue

Published on 01 April 2015. Downloaded by University of Illinois at Chicago on 08/05/2015 23:20:35.

Cite this: *Nanoscale*, 2015, **7**, 7559

Received 7th January 2015,
Accepted 27th March 2015

DOI: 10.1039/c5nr00095e

www.rsc.org/nanoscale

Charged group surface accessibility determines micelleplexes formation and cellular interaction†

Yu Zhang,[a] Yang Liu,[b] Soumyo Sen,[c] Petr Král[c,d] and Richard A. Gemeinhart*[a,e,f]

Micelleplexes are a class of nucleic acid carriers that have gained acceptance due to their size, stability, and ability to synergistically carry small molecules. MicroRNAs (miRNAs) are small non-coding RNA gene regulator that is consists of 19–22 nucleotides. Altered expression of miRNAs plays an important role in many human diseases. Using a model 22-nucleotide miRNA sequence, we investigated the interaction between charged groups on the micelle surface and miRNA. The model micelle system was formed from methoxy-poly(ethylene glycol)-*b*-poly(lactide) (mPEG-PLA) mixed with methoxy-poly(ethylene glycol)-*b*-poly(lactide)-*b*-oligoarginine (mPEG-PLA-R_x, x = 8 or 15). Surface properties of the micelles were varied by controlling the oligoarginine block length and conjugation density. Micelles were observed to have a core–shell conformation in the aqueous environment where the PLA block constituted the hydrophobic core, mPEG and oligoarginine formed a hydrophilic corona. Significantly different thermodynamic behaviors were observed during the interaction of single stranded miRNA with micelles of different surface properties, and the resulting micelleplexes mediated substantial cellular association. Depending upon the oligoarginine length and density, micelles exhibited miRNA loading capacity directly related to the presentation of charged groups on the surface. The effect of charged group accessibility of cationic micelle on micelleplex properties provides guidance on future miRNA delivery system design.

Over the last decade, miRNA has attracted significant attention due to their critical gene regulatory function in both normal biological process as well as various human diseases.[1] Micelleplexes, complexes formed by binding miRNA to micelles, have been designed for miRNA delivery. To form micelleplexes, miRNA is loaded onto the corona of the pre-formed micelles through multivalent ionic interactions.[2–8] Micelleplexes provide control over particle size through the hydrophobic interactions of the core and hydrophilic stability through the corona. To further develop and optimize micelleplexes for miRNA delivery, we sought to better understand the physical events driving micelleplex formation, structure, and stability. Despite the fact that block copolymer micelles properties have been relatively well studied, little has been described for the processes driving micelleplexes formation and stabilization. For the first time, the effects of charged group surface presentation on miRNA binding are investigated from a thermodynamic standpoint to improve the understanding of the interactions of miRNA with micelles.

Modification of the surface of nanoparticles has significant effect on the stability and biologic interactions of the nanoparticles.[9–11] To promote miRNA-micelle interactions, surface-exposed charged groups have been placed on micelles.[2] Unfortunately, the hydrophilic corona-forming components of micelles also tend to interfere with the binding of miRNA. The hydrophilic corona-forming components, generally poly(ethylene glycol) (PEG), form a 'hydration shell' on nanoparticles excluding the adsorption of proteins resulting in steric stabilization of the micelle.[12] Even with this shell, it is clear that proteins interact with the surface of micelles and other nanoparticles.[13–19] However, PEG on the surface also impairs cationic polymer interactions with nucleic acids due to decreased positive charge density, hydrogen bonding, and steric hindrance.[20,21] Moreover, once the micelleplexes arrive at targeted site, PEG is expected to diminish micelleplex-cell interactions, reducing cellular uptake of the micelleplexes resulting in a significant decrease in miRNA activity.[22,23] Design criteria that aid in the balance between binding of miRNA and steric stabilization would greatly improve the efficiency of micelleplex design.

[a]*Department of Biopharmaceutical Sciences, University of Illinois, Chicago, IL 60612, USA. E-mail: rag@uic.edu*
[b]*Department of Medicinal Chemistry and Pharmacognosy, University of Illinois, Chicago, IL 60612, USA*
[c]*Department of Chemistry, University of Illinois, Chicago, IL 60607, USA*
[d]*Department of Physics, University of Illinois, Chicago, IL 60607, USA*
[e]*Department of Bioengineering, University of Illinois, Chicago, IL 60607, USA*
[f]*Department of Ophthalmology and Visual Sciences, University of Illinois, Chicago, IL 60612, USA*

† Electronic supplementary information (ESI) available: Experimental procedures and additional supporting data, specifically the ^{1}H NMR spectra, micelle particle size, ζ-potential, CMC, and thermodynamic parameters of ITC. See DOI: 10.1039/c5nr00095e

Published on 01 April 2015. Downloaded by University of Illinois at Chicago on 08/05/2015 23:20:35.

To elucidate the effect of charged group surface presentation of micelles on miRNA loading, stability and cellular uptake, we engineered polymeric micelles that are composed of hydrophilic oligoarginine (R_x, x = 8 or 15) conjugated directly to the hydrophobic block of the mPEG-*b*-PLA block copolymer forming a triblock copolymer, mPEG-PLA-R_x[8] based upon our previous experience with the R_8 oligoarginine,[24] the expected extended lengths of the oligoarginine and poly(ethylene glycol), and previously published research.[8,25] We hypothesized that the mPEG-PLA-R_x micelles would present the oligoarginine block exposed on the surface, dependent upon the length of the oligoarginine block and the poly(ethylene glycol) block. An alternative structure where the oligoarginine block were placed on the poly(ethylene glycol) block, PLA-PEG-R_x, could also be examined and will be in the future to determine if these structures are presented as described for poly(lysine)[26,27] or oriented toward the interior of the structure.[10] Further, we hypothesized that the surface presentation of the oligoarginine would influence the miRNA-oligoarginine interactions and cellular uptake. In this way, the charged group was accessible for loading after formation, but the presentation at the surface could be controlled, unlike systems that bury the charged groups during the formation of the micelle and limit the loading to the point of formation of the particles.[28]

Micelles, mPEG-PLA-R_8, mPEG-PLA-R_{15}^{Low}, and mPEG-PLA-R_{15}^{High}, with arginine block conjugation density (proportion of oligoarginine modified triblock copolymer to total mPEG-PLA polymer) of 27%, 14% and 28% (mol%), respectively (Fig. 1A), were synthesized by coupling mPEG-PLA with CR_x through disulfide bond exchange reaction and purified with a Sep-Pak C_{18} column and characterized with ^{1}H NMR (Fig. S1†). For the purpose of easily distinguishing 14% and 28% R_{15} substituted mPEG-PLA-R_{15} micelles, we denote them as mPEG-PLA-R_{15}^{Low} and mPEG-PLA-R_{15}^{High}, respectively. All of the mPEG-PLA-R_x copolymers have similar critical micelle concentration (CMC) to the mPEG-PLA polymer (Fig. S2†). The micelles from each group had similar diameter (Table S1†). The ζ-potential of mPEG-PLA-R_8 micelles (30.76 ± 1.16) was similar to mPEG-PLA-R_{15}^{High} (30.46 ± 1.88), suggesting that only a portion of the oligoarginine contributed directly to the surface charge of the micelles. This was further supported by the ζ-potential of mPEG-PLA-R_8 and mPEG-PLA-R_{15}^{High} micelles being higher than mPEG-PLA-R_{15}^{Low} micelles (19.65 ± 4.7). In this way, we produced micelles with similar size, oligoarginine content (mPEG-PLA-R_8 and mPEG-PLA-R_{15}^{Low}) and charge (mPEG-PLA-R_8 and mPEG-PLA-R_{15}^{High}). The morphology of mPEG-PLA-R_8, mPEG-PLA-R_{15}^{Low} and mPEG-PLA-R_{15}^{High} micelles and micelleplexes were observed with transmission electron microscope, all of which demonstrated spherical shape and size similar to DLS measurements (Fig. S3†).

To understand the conformation of the micelles, micelles were prepared in D_2O for solution-phase NMR analysis.[29–31] In this technique, the constituents in the aqueous phase are readily detected but the hydrophobic-phase constituents have repressed signature. In aqueous solution, the triblock mPEG-*b*-PLA-R_x polymers formed micelles where the PLA hydrophobic chains collapse, with a disappearance of the PLA proton peaks, to form a hydrophobic core while the PEG chains and the R_x block constitute a hydrophilic corona. While the PLA protons were not detected in D_2O, the terminal methoxyl protons (δ = 3.40, 3H) from mPEG chains (Fig. 1B), the δ methylene protons from arginine side chain (δ = 3.20, 2H) and the α proton (δ = 4.40, 1H, Fig. 1B)[8] in the peptide backbone of R_x blocks remained detectable in the ^{1}H NMR spectrum. The prominent peaks (δ = 4.7 ppm and δ = 3.7 ppm) correspond to the solvent and methylene proton of poly(ethylene glycol), respectively. Based upon atomistic molecular dynamics simulation (Fig. 2), the number of total copolymer monomers to produce a micelle with a size observed by DLS and TEM is between 60 and 100 monomers. Using this estimate and the neutral to slightly positive ζ-potential of the micelles, it would be expected that the number of charged phosphate groups would match those of the charged arginine groups, or be slightly below unity. Therefore, the number of oligoarginines and miRNA loading of the micelles was estimated (Table 1).

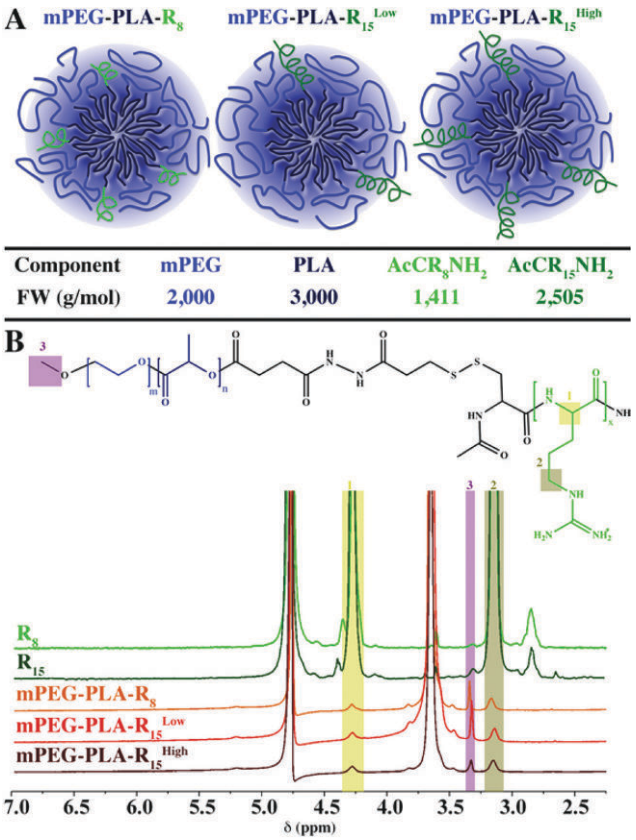


Fig. 1 Micelles properties and surface oligoarginine presence. (A) Schematic representation of the micelles formed and the relevant molecular weights of the components. (B) ^{1}H NMR analysis of the peptides (CR_8 and CR_{15}) and micelles (mPEG-PLA-R_8, mPEG-PLA-R_{15}^{Low}, and mPEG-PLA-R_{15}^{High}) showing the arginine α proton (1; δ = 4.40 ppm, 1H), δ protons (2; δ = 3.20 ppm, 2H), or ω-terminal methoxyl protons (arrow; δ = 3.40 ppm, 3H).

This journal is © The Royal Society of Chemistry 2015

Published on 01 April 2015. Downloaded by University of Illinois at Chicago on 08/05/2015 23:20:35.

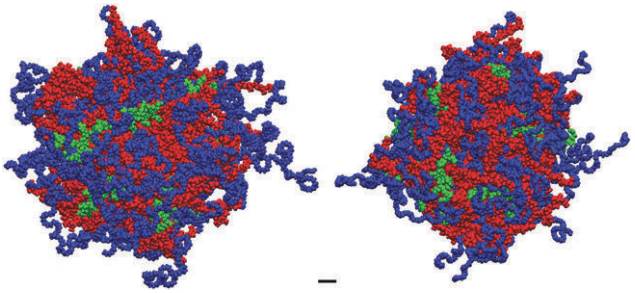


Fig. 2 Molecular dynamics simulation of mPEG-PLA-R_8 micelle. Each monomer consisted of a methoxy-poly(ethylene-glycol)(mPEG; MW ~ 2000 g mol^{-1}; blue) block coupled to the α-hydroxide of poly(lactide) (PLA; MW ~ 3000 g mol^{-1}; red). As in the experiments, 28% of total monomers were modified with oligoarginine (R_8; green) on the ω-carboxylate of the PLA block viewed along the x-y (right) and y-z (left) axes. The micelles were prepared with total 60 monomers.

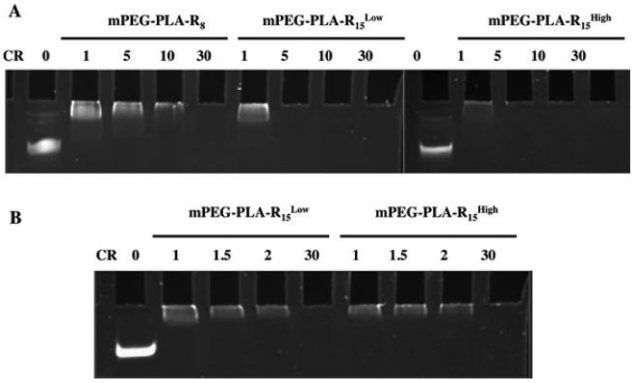


Fig. 3 MiRNA complexation with micelles occurs at lower charge ratios for longer oligoarginine regardless of oligoarginine density. (A) mPEG-PLA-R_8, mPEG-PLA-R_{15}^{Low}, and mPEG-PLA-R_{15}^{High} complexation with miRNA at +/− charge ratios of 1, 5, 10 and 30. (B) mPEG-PLA-R_{15}^{Low} and mPEG-PLA-R_{15}^{High} complexation with miRNA at +/− charge ratios 1, 1.5, 2 and 30.

Table 1 Estimates of the number of oligo-arginine peptides and miRNA associated with micelles

N_{agg} (copolymer[a]/micelle)	60		100	
N_Z (oligoargine/micelle or miRNA/micelle)	N_{R_x}	N_{miRNA}	N_{R_x}	N_{miRNA}
mPEG-PLA-R_8	16	6	27	10
mPEG-PLA-R_{15}^{Low}	8	6	14	10
mPEG-PLA-R_{15}^{High}	17	11	28	20

[a] Copolymers include both mPEG-PLA and mPEG-PLA-R_x. As presented in Table S1, 14, 27, and 28% of copolymers contain the arginine group for the mPEG-PLA-R_8, mPEG-PLA-R_{15}^{Low}, mPEG-PLA-R_{15}^{High} micelles, respectively.

These observations combined suggest the presence of oligoarginine block on the micelles surface, *i.e.* the aqueous phase. Based upon this, each of the micelles presented a portion of the oligoarginine on the surface with access to the aqueous environment.

Being present in the aqueous phase, however, does not indicate that the oligoarginine is free to interact with biomolecules in the presence of the PEG corona. To determine the ability of the micelles to interact with miRNA, the gel shift assay was conducted (Fig. 3A). mPEG-PLA-R_8 micelles were able to fully retard miRNA mobility only at or above a positive to negative (+/−) charge ratio (arginine to nucleotide) of 30, while mPEG-PLA-R_{15}^{Low} and mPEG-PLA-R_{15}^{High} fully retarded miRNA mobility at a charge ratio of 5. The lower charge ratio needed to fully bind miRNA further suggested that the mPEG-PLA-R_{15} micelles contain arginine that is more accessible to the surface for biomolecular interactions. This is further supported by the fact that mPEG-PLA-R_{15}^{Low} micelles interact with the miRNA as efficiently as the mPEG-PLA-R_{15}^{High} despite the fact that there is approximately half the total arginine present. No significant difference was observed for miRNA interactions with mPEG-PLA-R_{15}^{Low} and mPEG-PLA-R_{15}^{High} at low charge ratios (Fig. 3B). Based upon the interactions with miRNA, the longer oligoarginine chains are able to more readily interact with biomolecules at the surface of the micelles regardless of overall charge, *i.e.* ζ-potential, of the micelle. This is consistent with observation that PEGylation of cationic polymers generally deteriorates a polymer's ability to interact with DNA and RNA.[21]

To better characterize the interactions and gain information about the events leading to miRNA-micelle interactions, thermodynamic analysis was utilized.[32–35] An initial endothermic peak was observed for mPEG-PLA-R_8, which suggests that a molecular rearrangement took place prior to the ionic interactions between the peptides and the miRNA (Fig. 4). Unlike mPEG-PLA-R_8, only exothermic processes were observed when miRNA interacts with mPEG-PLA-R_{15}^{Low} or mPEG-PLA-R_{15}^{High}. Only the shorter arginine-containing micelles, mPEG-PLA-R_8, had an unfavorable entropic contribution while all micelles exhibited favorable enthalpy energy (Table S3†). PEG chains are thought to develop a 'hydration shell' where water is structured in the local vicinity surrounding the micelles.[12,36] The entropic loss ($-T\Delta S > 0$) during miRNA binding to mPEG-PLA-R_8 process might result from the disturbance of the hydration shell surrounding mPEG-PLA-R_8 in conjunction with unfavorable conformational changes necessary to accommodate the miRNA chain. Because the longer oligoarginine peptides are more accessible, the unfavorable rearrangements and the disruption of the ordered water layer are not necessary to accommodate the miRNA. The interactions of mPEG-PLA-R_{15}^{Low} and mPEG-PLA-R_{15}^{High} with miRNA are very similar to hyperbranched polyethylenimine (PEI) interactions with double strand siRNA,[35] suggesting that arginine clusters on the micelle surface could interact with miRNA in similar manner to PEI.

The entropic energy that was needed to form the complexes was coupled with a lower number of arginines that could inter-

Published on 01 April 2015. Downloaded by University of Illinois at Chicago on 08/05/2015 23:20:35.

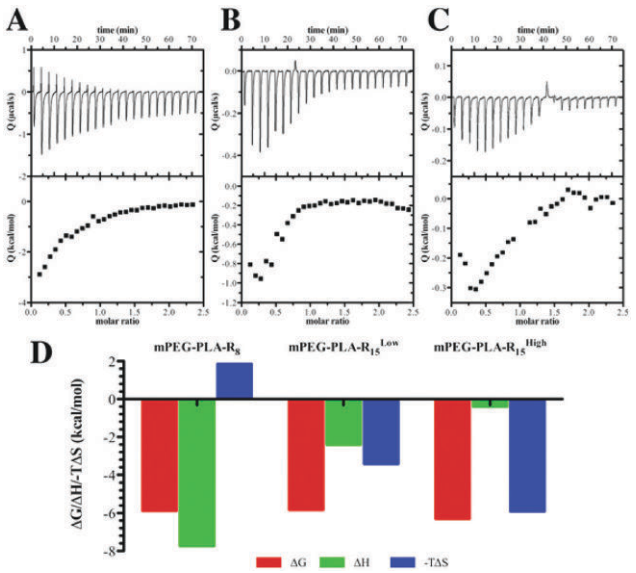


Fig. 4 Thermodynamic profiles of single stranded miRNA binding to micelles indicate different interactions occur dependent upon oligoarginine length and density. (A) mPEG-PLA-R_8 (B) mPEG-PLA-R_{15}^{Low} (C) mPEG-PLA-R_{15}^{High} (D) thermodynamic parameters, derived from ITC, of miRNA binding to mPEG-PLA-R_8, mPEG-PLA-R_{15}^{Low}, and mPEG-PLA-R_{15}^{High} micelles.

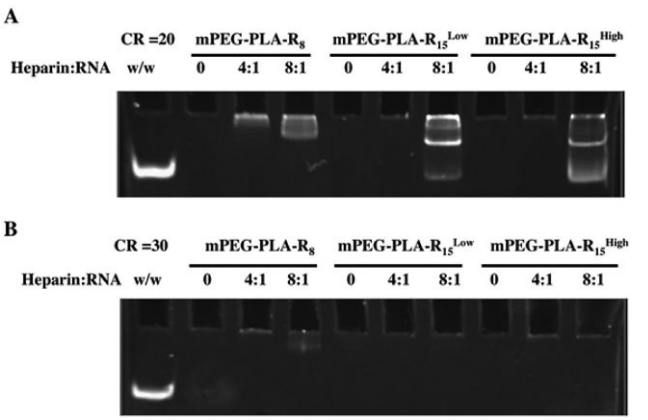


Fig. 5 Micelleplexes are stable to heparin competition. Micelleplexes were prepared at (A) +/− charge ratio 20 or (B) 30 and incubated with heparin at a heparin to miRNA weight ratio (w/w) of 0 : 1, 4 : 1, or 8 : 1 prior to electrophoresis and staining.

act with the miRNA. The mPEG-PLA-R_8 micelles only had about 2.6 arginines per peptide available to interact while the mPEG-PLA-R_{15}^{Low} and mPEG-PLA-R_{15}^{High} micelles had 6.2 or 11.0 arginines per peptide available to interact with miRNA, respectively. The differences in available arginines do not mirror the charge on the micelles (Table S2†), which were all positive, and the density of peptide being the only factor influencing the ζ-potential. This suggests that the available content of arginine increased on the surface as the amount of peptide in the micelles increased.

In addition to the role of the PEG corona shielding the charged groups during complexation, the PEG corona is also thought to influence the stability of the complexes by altering the surface accessibility of charged biomolecules, particularly anionic biomacromolecules that compete with negatively charged nucleic acids on the micelle surface. In all micelles, the micelleplex ζ-potentials were neutral compared to the original highly positive ζ-potential. Using the heparin sulfate competition assay to mimic the natural anionic macromolecules, shorter oligoarginine-containing micelles, mPEG-PLA-R_8, were not able to condense miRNA as tightly as longer oligoarginine containing micelles, mPEG-PLA-R_{15}^{Low} and mPEG-PLA-R_{15}^{High}. mPEG-PLA-R_x micelleplexes migrate in the polyacrylamide gel, but to a lesser extent than miRNA control due to the charge neutralization and the size of the micelleplexes (Fig. 3). At a charge ratio of 20, heparin did not dissociate miRNA from mPEG-PLA-R_8 micelles at a heparin to miRNA weight ratio of 4 : 1 (Fig. 5A), but based upon the diminished dye exclusion the miRNA appears to be less tightly bound to the micelleplex. The association between miRNAs and micelles was similarly loosened in mPEG-PLA-R_{15}^{Low} and mPEG-PLA-R_{15}^{High} micelleplexes in the presence of 8 : 1 heparin to miRNA. At a charge ratio of 30, heparin was unable to compete with miRNA or loosen the interactions. This suggests that the poorly accessible arginine content in mPEG-PLA-R_8 was less available for interactions, but once the interaction was formed the interaction was stable to heparin competition. mPEG-PLA-R_{15}^{Low} and mPEG-PLA-R_{15}^{High} have longer peptide sequence and appear to present a greater proportion of miRNAs closer to the surface than in mPEG-PLA-R_8 micelleplexes, and are thus less resistant to heparin competition. At a higher charge ratio of 30 to 1, all micelles were able to maintain the interaction with miRNA (Fig. 5B), suggesting that the interaction was stabilized with further ionic crosslinking. This observation agrees with others who observed that the macromolecules that freely interact with RNA are not necessarily the most stable.[37]

Finally, surface exposed charged groups on the micelles are believed to play key roles in their cellular interactions, with neutral particles (ζ-potential −10 to +10 mV) having limited non-specific cellular interactions.[10,38,39] mPEG-PLA-R_8 and mPEG-PLA-R_{15}^{High} micelles had higher ζ-potential than mPEG-PLA-R_{15}^{Low}, but the ζ-potential range of all three micelleplexes were generally neutral after miRNA complexation (Tables S1 and S2†). mPEG-PLA-R_{15}^{Low} and mPEG-PLA-R_{15}^{High} micelleplexes showed significantly more cellular association than mPEG-PLA-R_8 micelleplexes (Fig. 6). With the similar charge and size, the oligoarginine available on the micelle surface was expected to influence the ability of micelles to associate with or enter cells, but the total arginine and surface charge was not directly related to cellular interaction.[24,40,41] Only the available arginine content on the micelle surface correlated with the ability of the micelles to interact with cells. This further supports the idea that the oligoarginine on the mPEG-PLA-R_{15} micelles was more available for interactions.

In summary, we have presented the synthesis of triblock copolymers that form micelles and expose different amounts

 This journal is © The Royal Society of Chemistry 2015

Published on 01 April 2015. Downloaded by University of Illinois at Chicago on 08/05/2015 23:20:35.

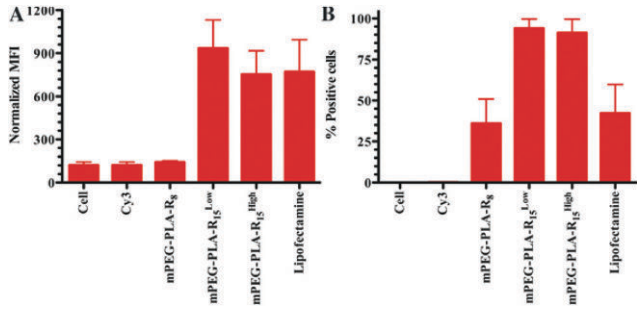


Fig. 6 Cellular association mediated by different micelleplexes. (A) The mean fluorescence intensity observed on U251 glioma cells following interaction with mPEG-PLA-R_8, mPEG-PLA-R_{15}^{Low}, and mPEG-PLA-R_{15}^{High} micelleplexes or untreated cells or Cy3-labeled miRNA. (B) The relative population (%) of cells associated with the mPEG-PLA-R_8, mPEG-PLA-R_{15}^{Low}, and mPEG-PLA-R_{15}^{High} micelleplexes or untreated cells or Cy3-labeled miRNA. N = 3, mean ± standard error of the mean.

of charged groups on their surface. We systematically studied the interactions of the micelles with miRNA and the miRNA-micelle complexes with biologic macromolecules and cells. By precise control of polymer structure, the accessibility of charged groups on micelle surface was used to control the interaction of miRNA with micelles and the eventual interaction with cells and the presence of oligoarginine near the hydrophobic core of the micelles was confirmed experimentally and through molecular modeling. The accessibility of the charged groups has direct impact on miRNA interaction with the micelles, micelleplexes stability and cellular interaction. These results guide the design of materials for RNA/DNA interactions by suggesting that the total charge of the groups used is not the primary factor for determining RNA binding or cellular association. Future work will further elucidate if the shielding of ionic groups can be controlled in alternate architectures. The PEG corona can shield the ionic groups thus diminishing RNA-micelle binding and minimizing cell binding; however, this PEG corona protects the RNA from competition yielding a more stable micelleplex.

Author contributions

The manuscript was written through contributions of all authors. All authors have given approval to the final version of the manuscript.

Funding sources

This investigation was conducted in a facility constructed with support from Research Facilities Improvement Program Grant Number C06 RR15482 from the National Center for Research Resources, NIH and funded by the UIC Center for Clinical and Translational Science (CCTS) award UL1 TR000050 (RAG), National Science Foundation award DMR 1309765 (PK), and Provost's Award for Graduate Research from UIC Graduate College (YZ). Yu Zhang was supported by University Fellowship from UIC.

Acknowledgements

The authors acknowledge Dr Hayat Onyuksel for generous sharing of instrumentation, Dr Gerd Prehna in University of Illinois at Chicago (UIC) Center for Structural Biology for assistance with ITC experiments and Dr Larry L. Klein for helpful discussion on polymer conjugation.

References

1 Y. Zhang, Z. J. Wang and R. A. Gemeinhart, *J. Controlled Release*, 2013, **172**, 962–974.
2 D. J. Gary, H. Lee, R. Sharma, J. S. Lee, Y. Kim, Z. Y. Cui, D. Jia, V. D. Bowman, P. R. Chipman, L. Wan, Y. Zou, G. Mao, K. Park, B. S. Herbert, S. F. Konieczny and Y. Y. Won, *ACS Nano*, 2011, **5**, 3493–3505.
3 Y. M. Kim and S. C. Song, *Biomaterials*, 2014, **35**, 7970–7977.
4 C. Q. Mao, J. Z. Du, T. M. Sun, Y. D. Yao, P. Z. Zhang, E. W. Song and J. Wang, *Biomaterials*, 2011, **32**, 3124–3133.
5 R. Sharma, J. S. Lee, R. C. Bettencourt, C. Xiao, S. F. Konieczny and Y. Y. Won, *Biomacromolecules*, 2008, **9**, 3294–3307.
6 T. M. Sun, J. Z. Du, Y. D. Yao, C. Q. Mao, S. Dou, S. Y. Huang, P. Z. Zhang, K. W. Leong, E. W. Song and J. Wang, *ACS Nano*, 2011, **5**, 1483–1494.
7 H. Yu, Y. Zou, Y. Wang, X. Huang, G. Huang, B. D. Sumer, D. A. Boothman and J. Gao, *ACS Nano*, 2011, **5**, 9246–9255.
8 Z. X. Zhao, S. Y. Gao, J. C. Wang, C. J. Chen, E. Y. Zhao, W. J. Hou, Q. Feng, L. Y. Gao, X. Y. Liu, L. R. Zhang and Q. Zhang, *Biomaterials*, 2012, **33**, 6793–6807.
9 R. M. Pearson, H.-j. Hsu, J. Bugno and S. Hong, *MRS Bull.*, 2014, **39**, 227–237.
10 R. M. Pearson, N. Patra, H. J. Hsu, S. Uddin, P. Kral and S. Hong, *ACS Macro Lett.*, 2013, **2**, 77–81.
11 L. Vukovic, F. A. Khatib, S. P. Drake, A. Madriaga, K. S. Brandenburg, P. Kral and H. Onyuksel, *J. Am. Chem. Soc.*, 2011, **133**, 13481–13488.
12 C. Allen, N. Dos Santos, R. Gallagher, G. N. Chiu, Y. Shu, W. M. Li, S. A. Johnstone, A. S. Janoff, L. D. Mayer, M. S. Webb and M. B. Bally, *Biosci. Rep.*, 2002, **22**, 225–250.
13 D. Pozzi, V. Colapicchioni, G. Caracciolo, S. Piovesana, A. L. Capriotti, S. Palchetti, S. De Grossi, A. Riccioli, H. Amenitsch and A. Lagana, *Nanoscale*, 2014, **6**, 2782–2792.
14 E. Casals, T. Pfaller, A. Duschl, G. J. Oostingh and V. Puntes, *ACS Nano*, 2010, **4**, 3623–3632.
15 T. Cedervall, I. Lynch, S. Lindman, T. Berggard, E. Thulin, H. Nilsson, K. A. Dawson and S. Linse, *Proc. Natl. Acad. Sci. U. S. A.*, 2007, **104**, 2050–2055.

Published on 01 April 2015. Downloaded by University of Illinois at Chicago on 08/05/2015 23:20:35.

16 H.-J. Hsu, S. Sen, R. M. Pearson, S. Uddin, P. Kral and S. Hong, *Macromolecules*, 2014, **47**, 6911–6918.
17 M. Lundqvist, J. Stigler, G. Elia, I. Lynch, T. Cedervall and K. A. Dawson, *Proc. Natl. Acad. Sci. U. S. A.*, 2008, **105**, 14265–14270.
18 M. P. Monopoli, D. Walczyk, A. Campbell, G. Elia, I. Lynch, F. B. Bombelli and K. A. Dawson, *J. Am. Chem. Soc.*, 2011, **133**, 2525–2534.
19 R. M. Pearson, V. V. Juettner and S. Hong, *Front. Chem.*, 2014, **2**, 108.
20 C. K. Chen, C. H. Jones, P. Mistriotis, Y. Yu, X. Ma, A. Ravikrishnan, M. Jiang, S. T. Andreadis, B. A. Pfeifer and C. Cheng, *Biomaterials*, 2013, **34**, 9688–9699.
21 R. E. Fitzsimmons and H. Uludag, *Acta Biomater.*, 2012, **8**, 3941–3955.
22 I. Endo, T. Nagamune and H. Akita, *Nano/Micro Biotechnology*, Springer, 2010.
23 H. Hatakeyama, H. Akita, K. Kogure and H. Harashima, *Adv. Biochem. Eng. Biotechnol.*, 2010, **119**, 197–230.
24 Y. Zhang, M. Köllmer, J. S. Buhrman, M. Y. Tang and R. A. Gemeinhart, *Peptides*, 2014, **58**, 83–90.
25 P. Liu, H. Yu, Y. Sun, M. Zhu and Y. Duan, *Biomaterials*, 2012, **33**, 4403–4412.
26 Y. Liu, Z. Chen, C. Liu, D. Yu, Z. Lu and N. Zhang, *Biomaterials*, 2011, **32**, 5167–5176.
27 Y. Liu, C. Liu, M. Li, F. Liu, L. Feng, L. Zhang and N. Zhang, *J. Biomed. Nanotechnol.*, 2014, **10**, 948–958.
28 H. X. Wang, X. Z. Yang, C. Y. Sun, C. Q. Mao, Y. H. Zhu and J. Wang, *Biomaterials*, 2014, **35**, 7622–7634.
29 L. Jongpaiboonkit, Z. Zhou, X. Ni, Y. Z. Wang and J. Li, *J. Biomater. Sci., Polym. Ed.*, 2006, **17**, 747–763.
30 A. S. Darefsky, J. T. King Jr. and R. Dubrow, *Cancer*, 2012, **118**, 2163–2172.
31 I. G. Shin, S. Y. Kim, Y. M. Lee, C. S. Cho and Y. K. Sung, *J. Controlled Release*, 1998, **51**, 1–11.
32 P. Holzerny, B. Ajdini, W. Heusermann, K. Bruno, M. Schuleit, L. Meinel and M. Keller, *J. Controlled Release*, 2012, **157**, 297–304.
33 L. Gu, L. M. Nusblat, N. Tishbi, S. C. Noble, C. M. Pinson, E. Mintzer, C. M. Roth and K. E. Uhrich, *J. Controlled Release*, 2014, **184**, 28–35.
34 L. B. Jensen, G. M. Pavan, M. R. Kasimova, S. Rutherford, A. Danani, H. M. Nielsen and C. Foged, *Int. J. Pharm.*, 2011, **416**, 410–418.
35 M. Zheng, G. M. Pavan, M. Neeb, A. K. Schaper, A. Danani, G. Klebe, O. M. Merkel and T. Kissel, *ACS Nano*, 2012, **6**, 9447–9454.
36 R. Kjellander and E. Florin, *J. Chem. Soc., Faraday Trans. 1*, 1981, **77**, 2053–2077.
37 S. Mao, M. Neu, O. Germershaus, O. Merkel, J. Sitterberg, U. Bakowsky and T. Kissel, *Bioconjugate Chem.*, 2006, **17**, 1209–1218.
38 C. Fortier, Y. Durocher and G. De Crescenzo, *Nanomedicine*, 2014, **9**, 135–151.
39 K. Xiao, Y. Li, J. Luo, J. S. Lee, W. Xiao, A. M. Gonik, R. G. Agarwal and K. S. Lam, *Biomaterials*, 2011, **32**, 3435–3446.
40 X. Xu, Y. Jian, Y. Li, X. Zhang, Z. Tu and Z. Gu, *ACS Nano*, 2014, **8**, 9255–9264.
41 Y. Liu, Y. J. Kim, M. Ji, J. Fang, N. Siriwon, L. I. Zhang and P. Wang, *Mol. Ther.–Methods Clin. Dev.*, 2014, **1**, DOI: 10.1038/mtm.2013.12.

 This journal is © The Royal Society of Chemistry 2015